Monte Carlo simulation of 3D nonvolatile memory

Yasuyuki Ohkura and Chikashi Suzuki

Semiconductor Leading Edge Technologies, Inc.
Onogawa, Tsukuba, Ibaraki, 305-8569 JAPAN
ohkura.yasuyuki@selete.co.jp

***Abstract*—3D fullband Monte Carlo simulator is applied to the analysis of floating gate injection current of nonvolatile memory. The simulation is performed with realistic number of particles, so the fluctuations due to the motion of particles in 3D device structure are discussed. By comparing the results with those by 2D calculation, the necessity of full 3D simulation both due to the capacitance coupling and particle fluctuation is shown to calculate read / write characteristics.**

Keywords-Fullband Monte Carlo, Nonvolatile memory, 3D effect

I. INTRODUCTION

The design of programming operation using channel hot electron injection is one of the important issues for the NOR type nonvolatile memory cell. There have been extensive investigations by fullband Monte Carlo simulation [1] [2] [3]. It has been shown to be important to consider high-energy electron distribution including carrier-carrier scattering [1] [4]. But in previous works, simulations have been done mainly by 2 dimensional (2D) analysis. As memory cells are getting so compact that 3 dimensional (3D) effects are becoming remarkable. Also carriers have electric charges, so Coulomb fluctuations occur with the movement of carriers. In the case of 2D analysis, each carrier correspond to a line charge, so Coulomb force is unnatural even if Plasmon and carrier-carrier scattering model is included [5]. Thus values of capacitances and drain and floating gate currents should be modified due to 3D effects.

In this paper, 3D Monte Carlo simulation of hot carrier injection effect is investigated. Fluctuations due to the motion of particles in 3D device structure are discussed. Finally 3D effects during programming operation are shown.

II. SIMULATION MODEL

Details of our fullband simulator, HyDeLEOSMC, with coupled Monte Carlo-drift diffusion method are described elsewhere [5]. Electron motions in the silicon channel region are modeled by MC method considering acoustic phonons, optical phonons, surface-roughness, impact-ionization and carrier-carrier scatterings, and transfer matrix method is used to calculate floating gate injection current.

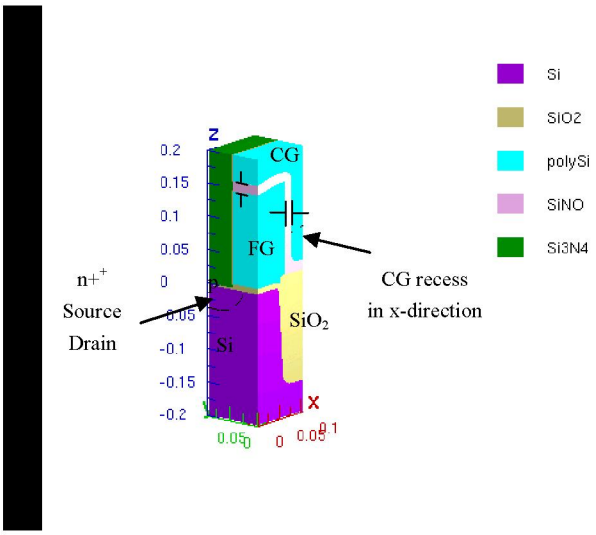

Figure 1. The quarter part of calculated memory cell structure

III. SIMULATION RESULT

In Figure 1, the simulated structure of a nonvolatile memory cell is shown, which is obtained by in-house process simulator HySyProS [6]. The size of floating gate (FG) is 90 nm in length and 110 nm in width, so number of electrons in the inversion layer under FG is about 1000 (when the inversion carrier density is 10^{13} cm^{-2}). So the realistic number of electron is used in our simulation.

In Figure 2, the calculated results of floating gate, source, and drain current (I_{FG}, I_{Sub} and I_D respectively) using HyDeLEOSMC are shown. In 3D analysis, the realistic number of electron is used. On the other hand in 2D analysis, sufficiently large number (about 50,000) of electrons is needed to suppress 'unnatural' potential oscillation. The values of 2D analysis are normalized by I_D ratio ($I_{D(3D)}$ / $I_{D(2D)}$), namely, by multiplying effective floating gate width (about 75 nm). I_{FG} and I_{Sub} in 3D analysis are relatively large compared with those in 2D analysis. The difference is mainly due to the plasma oscillation. Though the issue of double counting of short-range Coulomb force and 'mesh' force might be still remained, the difference represents adequate tendency. In the results of Figure 2, carrier-carrier and Plasmon scattering is not included.

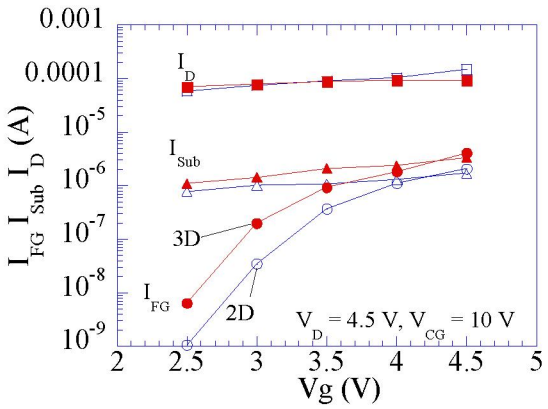

Figure 2. I_{FG}, I_{Sub}, I_D - V_{FG} characteristics of 3D (filled marks) and 2D (open marks) MC simulation. In 2D analysis I_G and I_{Sub} are normalized by $I_{D(3D)}$ / $I_{D(2D)}$.

The potential and particle distributions are shown in Figure 3 and 4 respectively as demonstrations of our results. In Figure 4, the carriers under the floating gate are treated as particles. Each globe in the center area of the figure corresponds to an electron, whose shading denotes its kinetic energy.

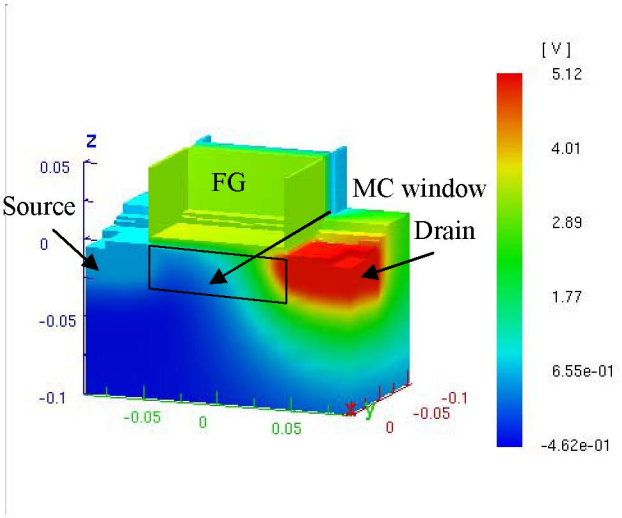

Figure 3. The potential distribution of 3D Monte Carlo simulation (V_D = 4.5 V, V_{FG} = 2.5 V).

In Figure 5, fullband calculations of floating gate current (I_{FG}) with and without carrier-carrier scattering (e-e) are compared in 2D. Floating gate currents increase including e-e. The difference is dominant at low V_{FG}, though drain currents are not so different. As in comparison with 2D and 3D results, both I_{Sub} and I_{FG} increases irrelevant to V_{FG}, the effect of carrier-carrier scattering is dominant only low V_{FG}, so the mechanism of the increase of the hot-carrier current in 3D is different from those of carrier-carrier scattering, though, due to huge computational burden, fullband calculation with carrier-carrier scattering in 3D is now under investigation.

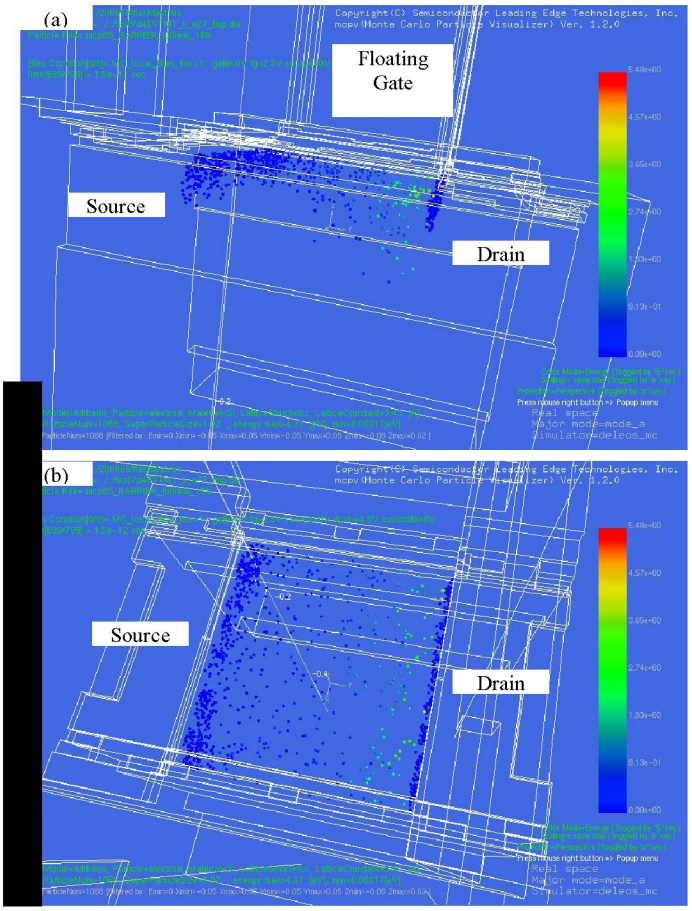

Figure 4. The distribution of particles under the floating gate of the nonvolatile memory at V_D = 4.5V, V_{FG} = 2.5 V, in which each particle corresponds 'one' electron, shown (a) from the side and (b) from the top (through the floating gate), respectively.

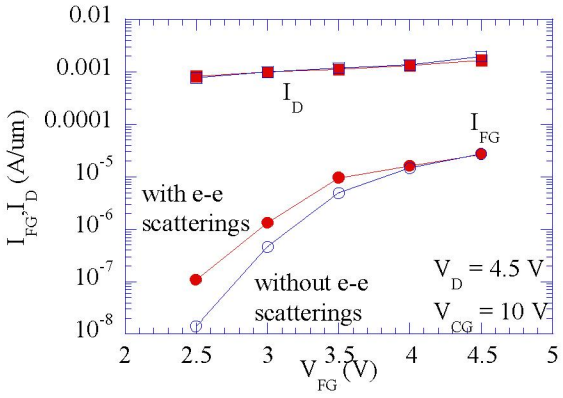

Figure 5. The effect of carrier-carrier scattering (e-e) on I_{FG} and I_D characteristics. Solid marks represent the result with e-e and open marks represent the result without e-e.

IV. Discussion on Fluctuation

In this chapter, the fluctuations due to the motions of particles in 3D device structure are discussed. First, the

transient number of particles in the Monte Carlo 'window' region is shown in Figure 6. In the figure, the number of particle is plotted every 2.5 fs. In simulation, particles are updated every 0.5 fs actually. The number becomes stable in 1 ps, as L_{FG} is 90 nm, thus the results between 1 ps and 2 ps are shown in the figure. The average number of particles is 1074.3 and its standard deviation is 9.7 at V_D = 4.5 V, V_{FG} = 2.5 V, which are statistically reasonable and realistic values.

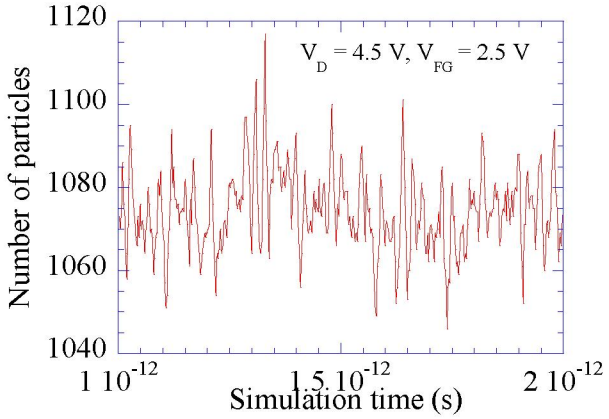

Figure 6. The transient number of particles in the Monte Carlo 'window' region.

In Figure 7, the snapshot of the potential distribution at the interface of silicon and oxide is shown. Equi-potential lines are not exactly parallel due to the fluctuation of the particles. The corresponding electron distribution is shown in Figure 8. In Figure 8, several 'needles' are shown which correspond to the particle location. The height of 'needles' represents the number of particles assigned to each grid.

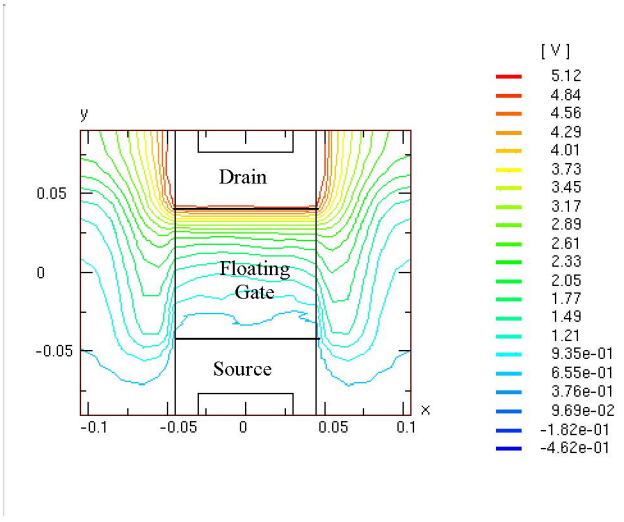

Figure 7. Potential distribution along silicon-oxide interface. V_D = 4.5V, V_{FG} = 2.5 V with 'realistic' electrons.

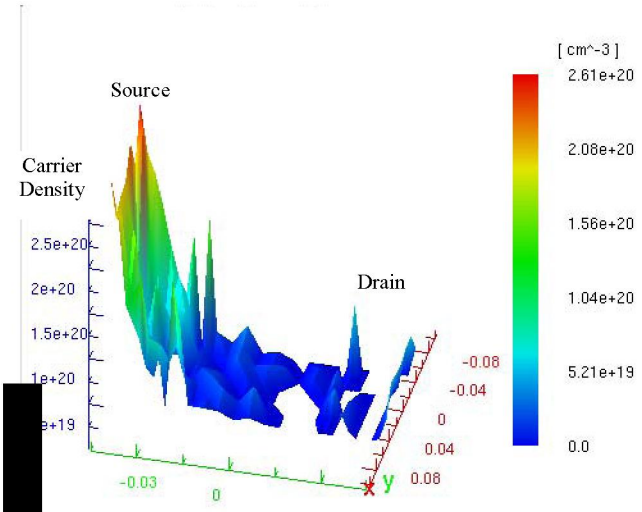

gure 8. Electron distribution along silicon-oxide interface. V_D = 4.5 V, V_{FG} 2.5 V with 'realistic' electrons. Electron concentration is assigned to each d.

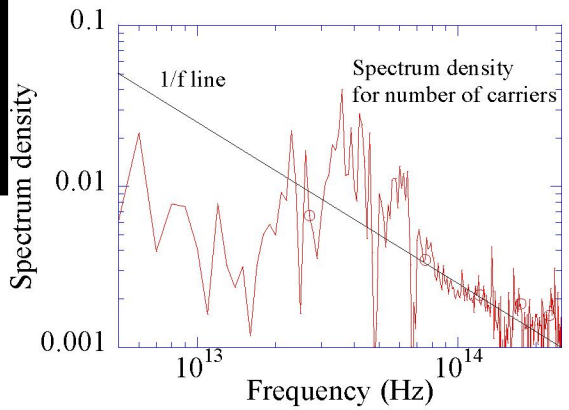

Figure 9. Specrum density of the number of carriers in the MC region. A line denotes 1/f characteristics.

In the Figure 9, the power spectral density functions $P(\omega)$ are shown, which are derived from the Fourier series of the auto-correlation functions for number of carriers shown in Figure 6. Here, autocorrelation function $C(\tau)$ is derived from Equation (1),

$$C(\tau) = \int_{t=t_0}^{t=t_{max}-\tau} \left(N(t) - \overline{N}\right)\left(N(t+\tau) - \overline{N}\right)dt \quad (1),$$

where t_0 is the initial integration time (we used 1ps) and t_{max} is the time when the simulation is ended. Then spectral density $P(\omega)$ is derived as Equation (2),

$$P(\omega) = \left| \int_0^{t_{max}-t_0} C(\tau)\exp(i\omega\tau)d\tau \right| / C(0) \quad (2)$$

Typical 1/f noise spectrum is observed in Figure 9. But any resonant peak due to plasma oscillation is not clearly

observed. Probably because plasma oscillation depends on local carrier densities in the range of Debye length, and its frequency is as small as 1 fs, plasma oscillation hardly affects the number of particles.

Anyway, there are fluctuations, which maybe enhance the hot carrier currents (I_{Sub} and I_{FG}) in 3D. More detail is now under investigation.

V. Programming Characteristics

Here, programming characteristics are discussed. Programming characteristics are important for improving the performance of nonvolatile memories. In measurements, the time shift of threshold voltage of control gate (V_{th_CG}) is evaluated, because of the difficulty of measuring V_{FG} and Q_{FG} directly. On the contrary, in simulation, user of the simulator can give V_{FG} and Q_{FG}, thus, the values of V_{th_CG} are derived from the I_D-V_{CG} characteristics in the read condition as functions of V_{FG} and Q_{FG}.

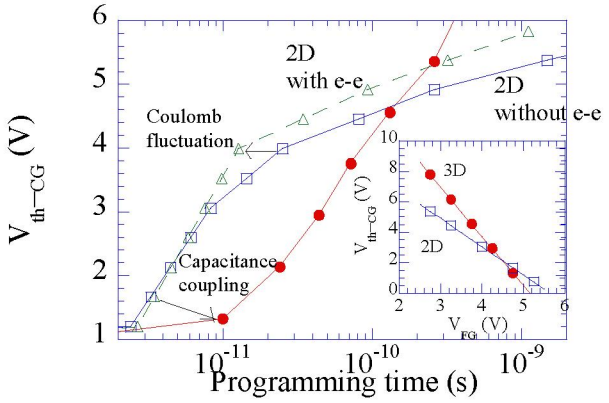

Figure 10. The programming characteristics with full 3D simulation (circles), and 2D simulation with (triangles) / without (squares) / carrier-carrier (e-e) scattering. The relations between V_{th_CG} and V_{FG_write} in 3D and 2D analyses are shown in the inset.

In Figure 10, programming transients of V_{th_CG} are shown. The solid curve represents the result of 3D simulation (circles), and 2D simulation with (triangles) / without (squares) carrier-carrier (e-e) scattering respectively. In the programming operation, the biases are applied as V_D = 4.5 V and V_{CG} = 10 V. In MC simulation, $I_{FG}(V_{FG})$ is calculated, and then, programming times are derived from Equation (3),

$$dt = \{1 / I_{FG}(V_{FG})\}\, dQ_{FG}$$
$$= \{1 / I_{FG}(V_{FG})\}\, C_{FG\text{-}CG}(V_{th\_CG})\, dV_{th\_CG} \quad (3),$$

where, V_{th_CG} is the threshold voltage defined at read operation (I_D / W_{FG} = 10 nA / um and V_D = 1 V), and

$$C_{FG\text{-}CG}(V_{th\_CG}) = dQ_{FG} / dV_{th\_CG}.$$

Remarkable difference is observed between 2D and 3D simulation. There are two reasons for the difference.

1) Capacitance coupling: As shown in Figure 1 due to the recess of CG in the x-direction, the capacitance coupling is stronger in 3D compared to that in 2D ($C_{FG\text{-}CG(3D)} > C_{FG\text{-}CG(2D)} * W_{FG}$). Thus the relation between V_{th_CG} and V_{FG_write} are modified due to the difference of capacitance coupling, which are shown in the inset of Figure 10.

2) Coulomb fluctuation: Programming time mainly depends on I_{FG} around the final V_{FG}, where I_{FG} increase due to the increase of hot carrier distributions by Coulomb fluctuations. Thus, the increase of I_{FG} due to Coulomb fluctuation is one of key factors. The difference has been shown in Figure 2. Also, as the effects of Coulomb fluctuations by carrier-carrier scattering and Plasmon scattering on potential distributions are difficult to separate from other Coulomb effects in 3D analysis, 2D simulation with and without carrier-carrier scattering are shown as references.

VI. Conclusion

In conclusion, programming characteristics of a NOR type nonvolatile memory are calculated by a fullband Monte Carlo simulator. As the effect of Coulomb force is important to the hot carrier injection, so simulation with 3D structure and realistic number of carriers is desired. The increase of floating gate injection current due to Coulomb force is shown.

Fluctuations due to the motion of particles in 3D device structure are discussed. Power spectral density function is derived. Typical 1/f noise spectrum is observed.

3D analysis and 2D analysis are compared. Not only 3D effects of capacitance coupling but also the increases of floating gate current due to 3D Coulomb fluctuation are key factors for accurate design of memory cell.

References

[1] J. D. Bude, M. R. Pinto and R. K. Smith, "Monte Carlo simulation of CHIESEL Flash memory cell," IEEE Trans. Electron Devices, 47, pp. 1873-1881 (2000).

[2] D. R. Nair, S. Mahapatra, S. Shukuri and J. D. Bude, "Drain Disturb During CHISEL Programming of NOR Flash EEPROMs—Physical Mechanisms and Impact of Thechnological Parameters," IEEE Trans. Electron Devices, 51, p. 701-707 (2004).

[3] D. Esseni and L. Selmi, A. Ghetti and E. Sangiorgi, "A better understanding of substrate enhanced gate current in MOSFETs and Flash cells—Part I: Phenomenological aspects," IEEE Trans. Electron Devices, 46, p. 369-375 (1999).

[4] M. V. Fischetti and S. E. Laux, "Monte Carlo Study of Electron Transport in Silicon Inversion Layers", Phys. Rev. B, 48, pp. 2244-2274, (1993).

[5] Y. Ohkura, C. Suzuki, T. Enda, H. Takashino, H. Ishikawa, T. Kojima and T. Wada, "A 3-dimensional particle device simulator; HyDeLEOSMC and its application to a FinFET," SISPAD 2005, pp. 287-290.

[6] T. Wada and N. Kotani, "Design and Development of 3-Dimensional Process Simulator," IEICE Trans. Electron., E82-C, pp. 839-847 (1999).

[7] Y. Ohkura, C. Suzuki, H. Amakawa and K.Nishi, "Analysis of gate currents through High-K dielectrics using a Monte Carlo Device Simulator", SISPAD 2003, pp. 67-71.